ADVANCED LASER SCANNER FOR THE SIMULATION OF COSMIC RAY EFFECTS ON MICROELECTRONIC DEVICES

Final Report

JPL 730-00492-0-5140

Quiesup Kim, JPL
George A. Soli, JPL

A. OBJECTIVES

The objective of this task was to demonstrate the cost-effective and nondestructive capabilities of the advanced laser scanner for simulation of cosmic ray upsets in microelectronics. Acquisition of laser-determined parameter data will enable quantification of the variables associated with single-event upsets (SEUs). By adjusting laser parameters such as wavelength and power, the upset threshold energies for various devices were determined. These data will then broaden the understanding of SEUs and provide the basis for innovative protection schemes.

Space applications of microelectronic integrated circuits (ICs) require that their susceptibility to SEUs be determined prior to insertion into the space system. To best simulate the space environment, SEU testing is normally done at a large accelerator capable of producing a beam of high-energy heavy ions. However, these tests are difficult, time consuming, and expensive to perform. And, although an accelerator may provide ions more like those in space, the information obtained is limited in certain important respects. For example, the entire chip is exposed to the particle beam, eliminating the possibility of isolating particularly sensitive regions within the circuit. The technique described here addresses these objectives and provides a powerful, alternative technique for studying SEUs.

B. PROGRESS AND RESULTS

1. Experimental Results

A picosecond pulsed dye laser beam operated at selected wavelengths was successfully used to simulate SEUs in N-type metal-oxide-silicon (NMOS) dynamic random-access memories (DRAMs). The DRAM upset levels were compared with published ion data. The diffusion model of laser upsets in an NMOS DRAM fits ion-beam upset data within a factor of two. Results indicate that the technique can be directly used not only for prescreening devices, but also to help properly design radiation-hardened devices for space applications.

Although similar SEU laser simulation systems have been described elsewhere [1,2,3], the system in use at JPL (Figure 1) is the only one that employs a dye laser. This has many advantages for SEU simulation, including the ability to easily tune the laser over a significant range of wavelength values. Because the absorption coefficient of silicon varies strongly with wavelength, the tunability allows one to perform an approximate depth profile of SEU sensitivity. The light-assisted microelectronic advanced laser scanner (LAMEALS) is based on a dye laser with a pulse duration of less than 20 ps, which is sufficient for SEU simulation, and a focused beam size of 1.5 μm, small enough to isolate sensitive devices on the chip. Combining the laser with computer image processing allows the precise location of the laser probe beam on the IC chip, e.g., on access transistors or storage capacitors. Selection of the laser wavelength then determines the specific location and depth range of the laser threshold upset energy, which can be converted to an effective linear-energy transfer (LET).

To simulate the laser technique, the Micron Technology MT1259 was selected; it is a 256K × 1 dynamic NMOS RAM. This device has four cell arrays, each consisting of 128 rows × 512 columns of cells (see Figure 2). Each cell consists of an access transistor and a storage capacitor. These DRAMs were chosen because heavy-ion SEU data from

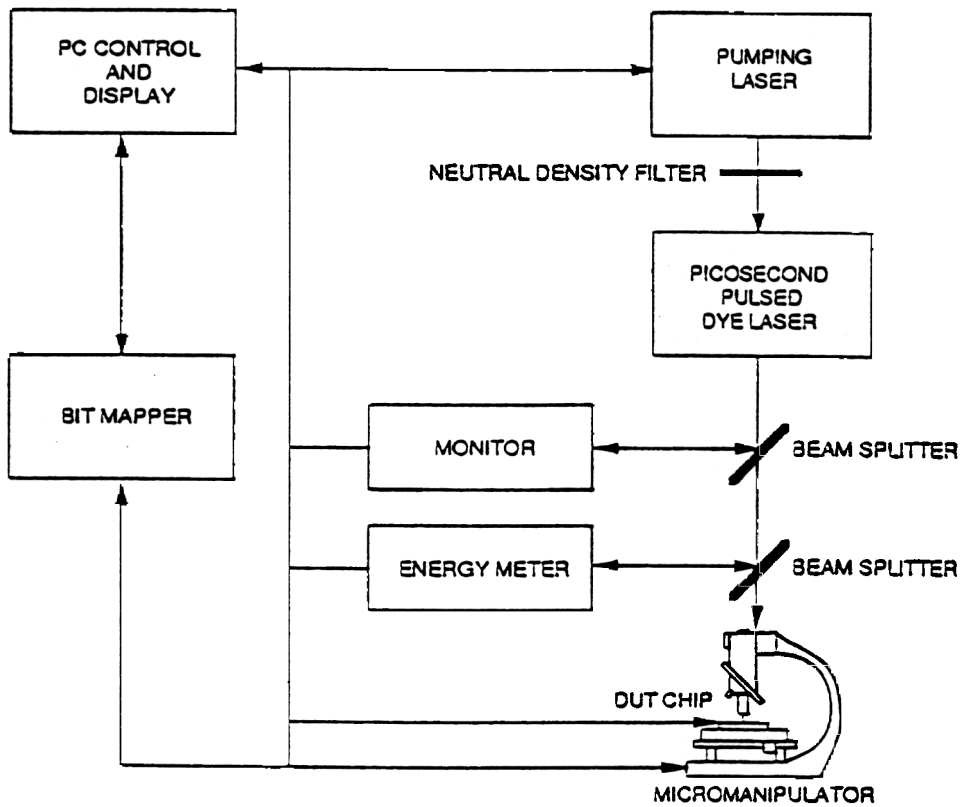

Figure 1. Experimental setup for picosecond dye laser to simulate cosmic ray effects.

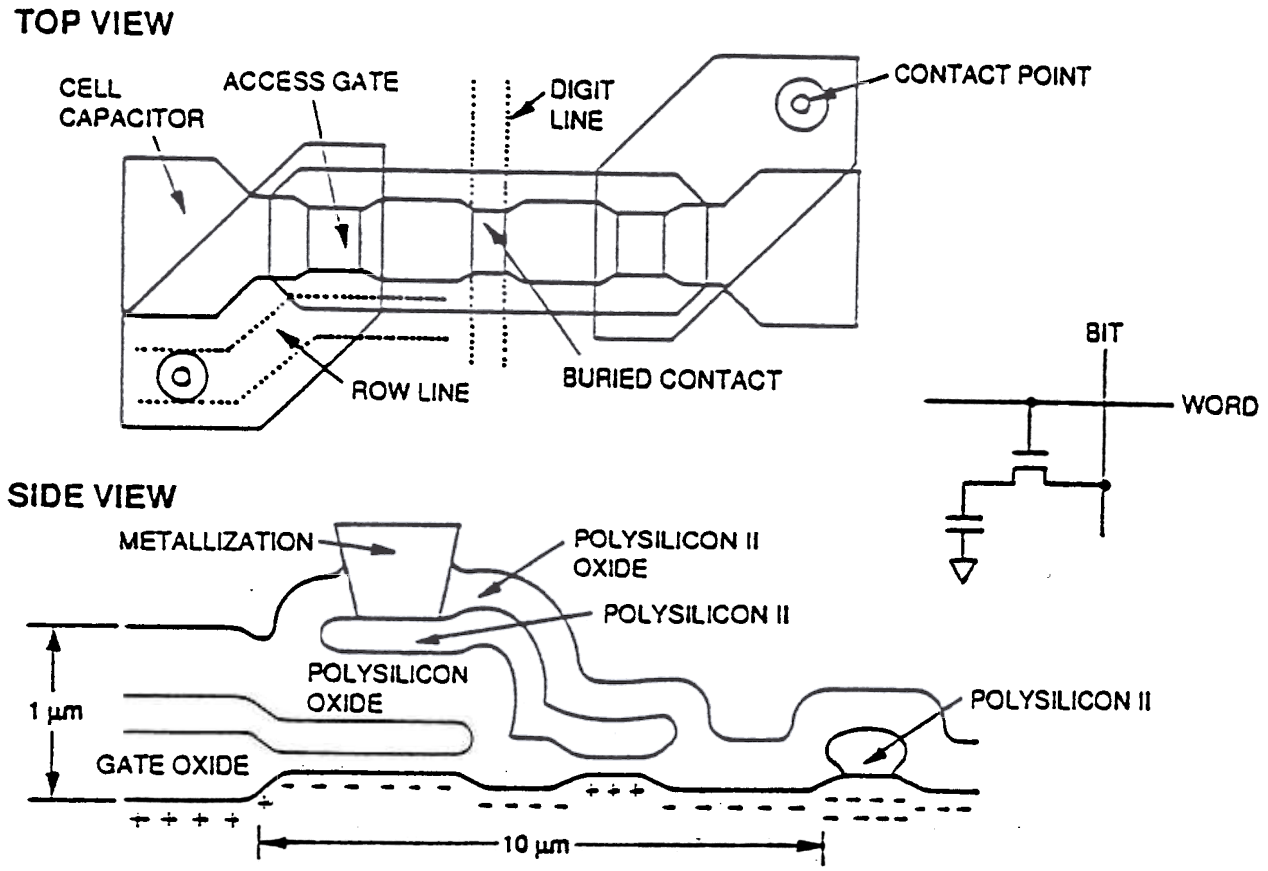

Figure 2. Schematic diagram of 256K NMOS DRAM (MT1259).

the Berkeley 88-inch accelerator already existed [4,5,6]. The devices were scanned with the laser probe beam while varying the laser energy and wavelength between 500 and 900 nm. Figure 3 shows the size of the laser beam relative to the important components of the DRAM cells. Note that the beam diameter of the laser can be easily isolated on a particular component.

Two tests are possible: sensitive, in which all cells are charged to the one state, and insensitive, in which they are discharged to the zero state. Bit-mapped images of events occurring in the device under test (DUT) are provided by bit-mapping software in the test system, which reads the logical row and column data collected from the DUT card and translates them into physical row and column addresses.

Examples of upset bit maps of DRAM operating at V_{DD} of 5.0 V, which have been obtained using a laser wavelength of 688 nm, are shown in Figures 4a and 4b. A dot at the head of the arrow in Figure 4a shows an upset memory cell located at the 312th column in the 115th row. The pattern of upset bits shown in Figure 4b

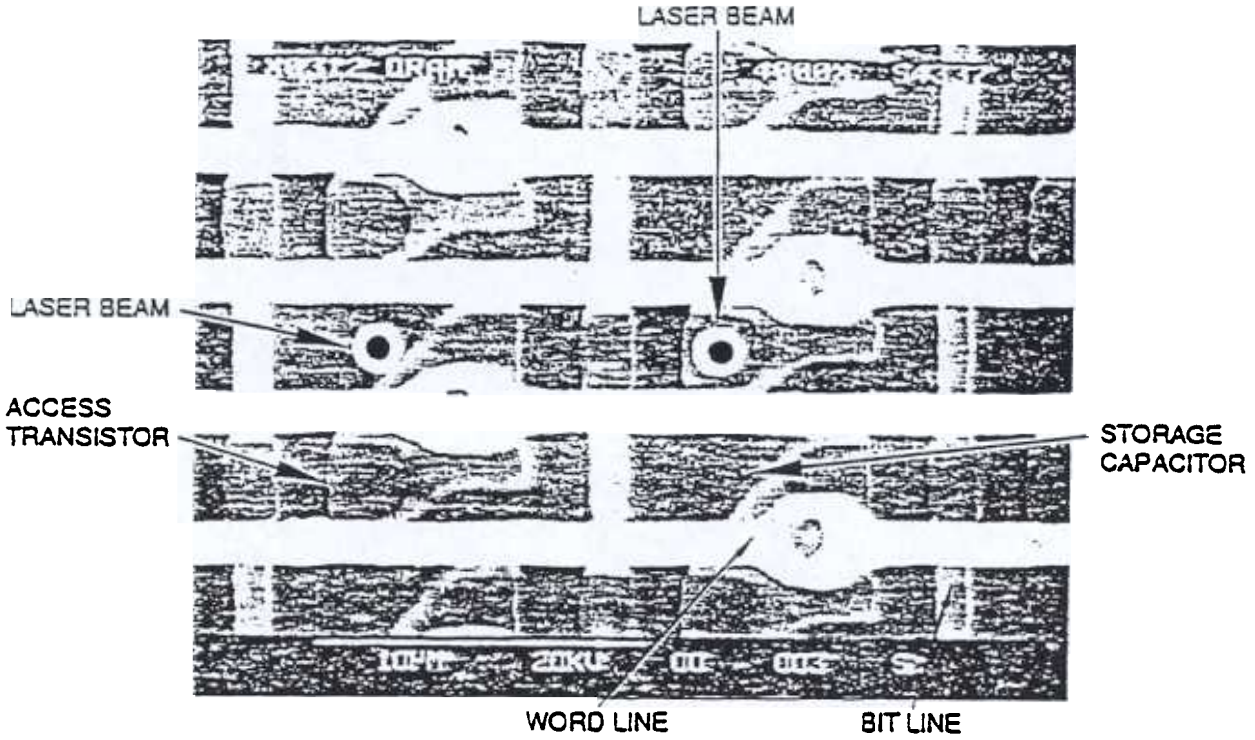

Figure 3. Comparison of laser beam sizes with active components.

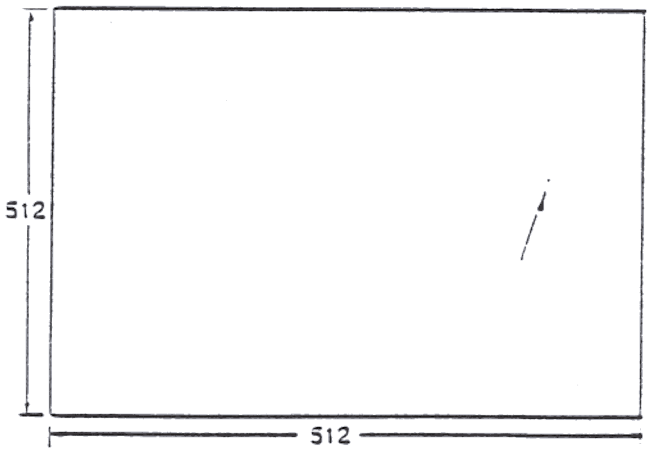

Figure 4a. An optical bit map of a single-pulse irradiation on a storage capacitor of NMOS DRAM (MT1259).

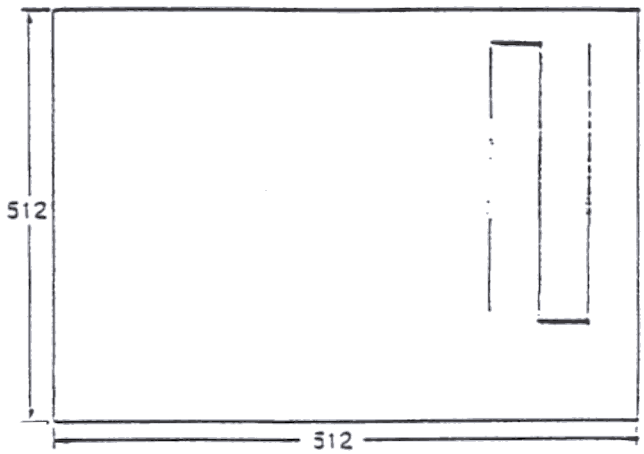

Figure 4b. An optical bit map plotted by the scanning LAMEALS on a 256K NMOS DRAM (MT1259).

demonstrates the scanning capability of the system. In this mode the microscope is automatically moved after each laser pulse.

The data in Table 1 show the different effects caused by the location and wavelength of the laser. At each wavelength, the upset rate for the storage capacitor is normalized to that for the access transistor. Data presented in this fashion are not meant to suggest that the upset rate of the access transistor is independent of wavelength. Note that the upset rates are about the same for the two components at 652 nm, but that at the more deeply penetrating wavelength of 724 nm, the storage capacitor upset rate is much less than that for the access transistor. While detailed explanation of this result awaits further experimentation and analysis, the reduced upset rates of the storage capacitor at longer wavelengths agrees with what one might expect. That is because the more deeply penetrating 724-nm light deposits a smaller fraction of its energy near the capacitor-sensitive region. In any case, Table 1 indicates that the laser has the potential for revealing important information about upsets in ICs not easily available with heavy-ion tests.

Table 1. Relative Upset Rates for Different Components of the DRAM

Laser Wavelength (nm)	652	688	724
Access Transistor	1.00	1.00	1.00
Storage Capacitor	0.95	0.36	0.08

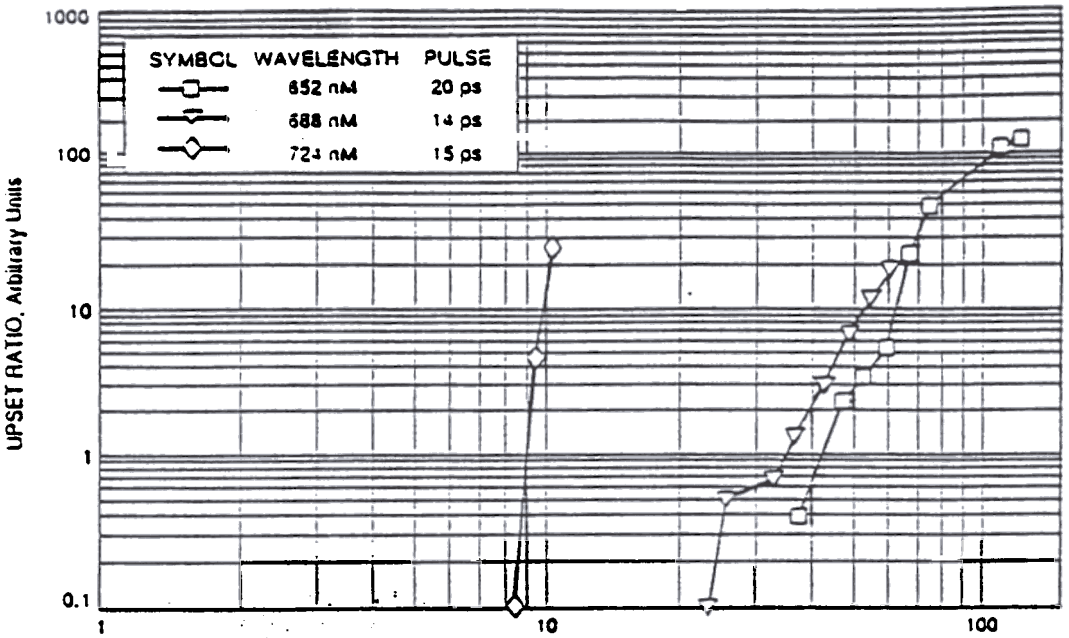

Figure 5. SEU counts versus the linear energy transfer of different laser pulses.

Figure 5 shows the upset counts at selected laser intensities and wavelengths of an MT 1259 access transistor. Energy, pulse height and duration, and repetition rate were adjusted to optimize device upsets operating at a V_{DD} of 5.0 V. The laser light was passed through a filter that absorbed either the infrared or visible light, as required, and neutral-density filters were used to attenuate the beam intensity to the required critical beam energy for upset. Finally, the beam was directed through a 100× microscope lens that focused down to less than a 1.5-μm-diameter spot incident on the circuit. Adjusting the microscope x-y stage allowed for easy positioning of a sensitive circuit node directly in the beam.

When using the infrared light, alignment was first achieved with visible light, then with filters changed to pass only infrared light. The transmittance of each optical element, including the focusing lens, was measured to determine the amount of energy incident on the circuit. Upset counts of NMOS DRAMs during irradiation by various wavelengths from the dye laser were monitored by a bit mapper. For the sensitive modes of the mapper, threshold-effective LETs at 724-, 688-, and 652-nm laser wavelengths were estimated to be 8.3, 23.0, and 37.2 MeV/mg/cm^2, respectively.

Effective laser LET was defined by

$$T/\Omega \; \delta/\delta Z \; \{P_{\mathcal{J}_0} \exp(-\alpha Z)\}$$

$$= \alpha \, T \, P_{\mathcal{J}_0} \exp(-\alpha Z) / \Omega$$

where T is a transmissivity factor, Ω is the molecular density of silicon, $\delta/\delta Z$ is a partial derivative of the vertical distance from the device surface Z, P_o is the incident laser power, t_o is the pulse duration, and α is the absorption coefficient. All the variables are statistical quantities, not dynamical. The threshold energy was determined by measuring the critical energy required to change any memory status. Note that the threshold linear energy transfer of an ion beam was reported to be ≈1 MeV [4].

An interesting phenomena observed in these tests were the optical-biasing effects on upsets in the nonsensitive mode, when the laser beam alone could not upset the memory. However when an optical bias of visual light of ≈20 kW/cm^2 was applied, the memory could be upset, as shown in Figure 6. The memory could also be upset by the high-intensity biasing light alone. This technique appears to be of important technical merit because it opens the LAMEALS to the failure diagnosis of microelectronic devices, including SEUs. Further study of this technique is under negotiation with the Defense Nuclear Agency and NASA (QE and QR).

2. Theoretical Modeling

The dominant charge transfer mechanism of either tunneling or diffusion determines which plasma-track characteristics are most relevant. Previous investigation by krypton ions has shown that charge collection in this device is via long-range diffusion [4,5,6]. Therefore, all plasma-track characteristics generated by the picosecond pulsed dye laser could be relevant and it is necessary to start from first principles to solve the transport equation. Analysis of other types of devices will be the subject of future work.

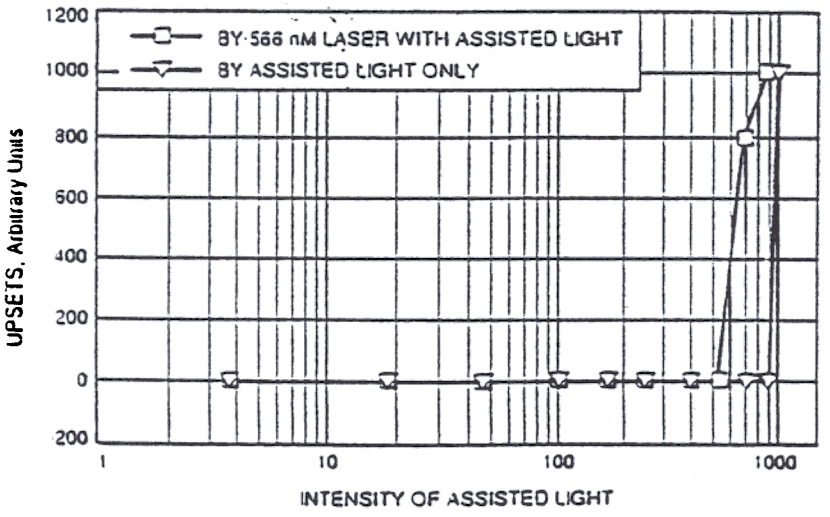

Figure 6. Upset counts of NMOS DRAM (MT1259, nonsensitive mode) by a 566-nm laser with assisted light and by assisted light only.

The carrier density P is assumed to satisfy the ambipolar diffusion equation

$$D^* \text{ div grad } P = (1/\tau + \delta/\delta t)\, P$$

where D^* is the ambipolar diffusion constant, τ is carrier lifetime and $\delta/\delta t$ is the partial derivative with respect to t. While the diffusion current can be calculated from P, the time-integrated current, or collected charge, can be calculated from the time integral of P. Hence it is convenient to define μ by

$$\mu = \int_0^\infty P(r,t)\, dt$$

where r is the junction distance from the track.

The equation governing μ is obtained by integrating Eq. (1) to get

$$D^* \text{ div grad } \mu - \mu/\tau = - P_I$$

where P_I is the initial ($t = 0$) carrier density. The plasma-track diameter is small compared to track-to-junction distances, and P_I will be approximated as a delta function in the lateral coordinates. The upper surface is represented as the x-y plane, so that Eq. (3) becomes

$$D^* \text{ div grad } \mu - \mu/\tau = - \delta(x)\, \delta(y)\, \sigma(z) \qquad (4)$$

where σ is the initial linear-track density, i.e., the initial number of electron-hole pairs per unit track length.

A junction will upset if the charge collected by the junction exceeds some threshold value, K_o. The collected charge is proportional to grad μ evaluated at the junction location and, therefore, an upset will occur if

$$\delta\mu/\delta z > K_o$$

where K_o is a threshold value that depends on device construction and bias voltage and measures device susceptibility. If K_o can be experimentally measured, an upset prediction can be made by analytically evaluating the left side of the above inequality and determining if the inequality is satisfied. An objective of the analysis to follow is to use laser data to determine K_o. However, K_o depends on bias voltage and it is convenient to separate this dependence. The critical charge, and therefore K_o, is expected to be

proportional to bias voltage ($K_o \equiv V_{DD} K$). Therefore, the condition for an upset can be rewritten as

$$\delta\mu/\delta z > V_{DD} K$$

where V_{DD} is a relative potential. It is the bias voltage divided by 5 V, which is an arbitrarily chosen reference bias voltage. K depends on device construction but is not expected to depend on bias voltage.

The upset radius is r_u, satisfying

$$\left.\frac{\delta\mu}{\delta z}\right|_{r=r_u,\ z=0} = V_{DD} K \tag{5}$$

Junctions within r_u distance from the track should upset, while the more distant junctions should not. Let N_u be the number of upsets and n the number of upsettable junctions per unit area. N_u is related to r_u by

$$N_u = \Pi\, n\, r_u^2 \tag{6}$$

It is necessary to evaluate the left side of Eq. (5). Reference [7] gives the infinite space Green's function for the modified Helmholtz equation. It is assumed that the combined effect of the charge-collecting junctions (including bit-line junctions) is similar to the effect produced when the entire upper surface is a sink ($\mu = 0$). This boundary condition is easily included using the method of images. The result is

$$\left.\frac{\delta\mu}{\delta z}\right|_{r=r_u,\ z=0} = (2\Pi D^* r_u)^{-1}\, \sigma(0)\, \exp[-r_u (D^* \tau)^{-1/2}]$$

$$+(2\Pi D^*)^{-1} \int_0^\infty \sigma'(u)(r_u^2 + u^2)^{-1/2} \exp[-(r_u^2 + u^2)^{1/2} (D^*\tau)^{-1/2}]\, du \tag{7}$$

where σ' is the derivative of σ.

In this analysis the only difference between lasers and heavy ions is the function σ. Assuming one electron-hole pair per 1.12 eV, σ is related to the laser pulse LET by

$$\sigma(z) = a_l\, L_o \exp(-\alpha z) \text{ for laser} \tag{8}$$

where

$$a_l = 2.08 \times 10^9 \text{ cm}^{-1} (\text{MeV–cm}^2/\text{mg})^{-1}$$

and L_o is the initial (z = 0) LET and α is the absorption coefficient. Because of σ' in Eq. (7), the exponential has an influence only when u is on the order of or less than $1/\alpha$. But, in the test data considered here, such values of u are small compared to $(D^* \tau)^{1/2}$ because $1/\alpha$ was small compared to the diffusion length. Therefore, u can be replaced with zero in the exponential function in Eq. (7). It is also helpful to use the approximation

$$(r_u^2 + u^2)^{-1/2} \approx r_u^{-1} - u^2 (2 r_u^3)^{-1}$$

Combining these approximations with Eqs. (5), (6), (7), and (8) gives

$$L_R = 2\Pi D^* K T \text{ for laser}$$

where

$$T \equiv a_1^{-1} \alpha^2 N_u^{3/2} (\Pi n)^{3/2} \exp [N_u^{1/2} (\Pi n D^* \tau)^{-1/2}]$$

$$L_R \equiv L_o / V_{DD}$$

For heavy ions, we assume that σ is constant for distance r, the track length, so that

$$\sigma = a_1 L_o \qquad 0 < z < r$$

where L_o is the LET at z = 0 and (assuming one electron-hole pair per 3.6 eV)

$$a_1 = 6.47 \times 10^8 \text{ cm}^{-1} (\text{MeV–cm}^2/\text{mg})^{-1}$$

Combining Eqs. (5), (6), (7), and (11) gives

$$L_R = 2\Pi D^* a_1^{-1} K S^{-1} \text{ for ion}$$

where

$$S = W_1^{-1} \exp[-W_1 (D^* \tau)^{-1/2}] - W_2^{-1} \exp [-W_2 D^* \tau)^{-1/2}] \qquad (12b)$$

$$W_1 \equiv [N_u / (\Pi n)]^{1/2} \qquad (12c)$$

$$W_t \equiv [N_t/(\Pi n) + r^2]^{1/2} \qquad (12d)$$

Experimental laser data is plotted in the form of T versus L_R where L_R is calculated from Eq. (10) and L_o is calculated from the total laser pulse energy E by

$$L_o = \alpha d^{-1} E$$

where d is the density of silicon. T is calculated from Eq. (9b) using $n = 2.24 \times 10^{-2}\ \mu^{-2}$. According to Eq. (9a), the graph should be a straight line with reciprocal slope $2\Pi D^{**}K$, which provides an experimental determination of K.

The actual graph is shown in Figure 7 and the raw data in Table 2. A great deal of scatter can be seen in the laser data. This is also true for heavy-ion data as shown in [5,6] which had to resort to histograms to characterize the device response to heavy ions

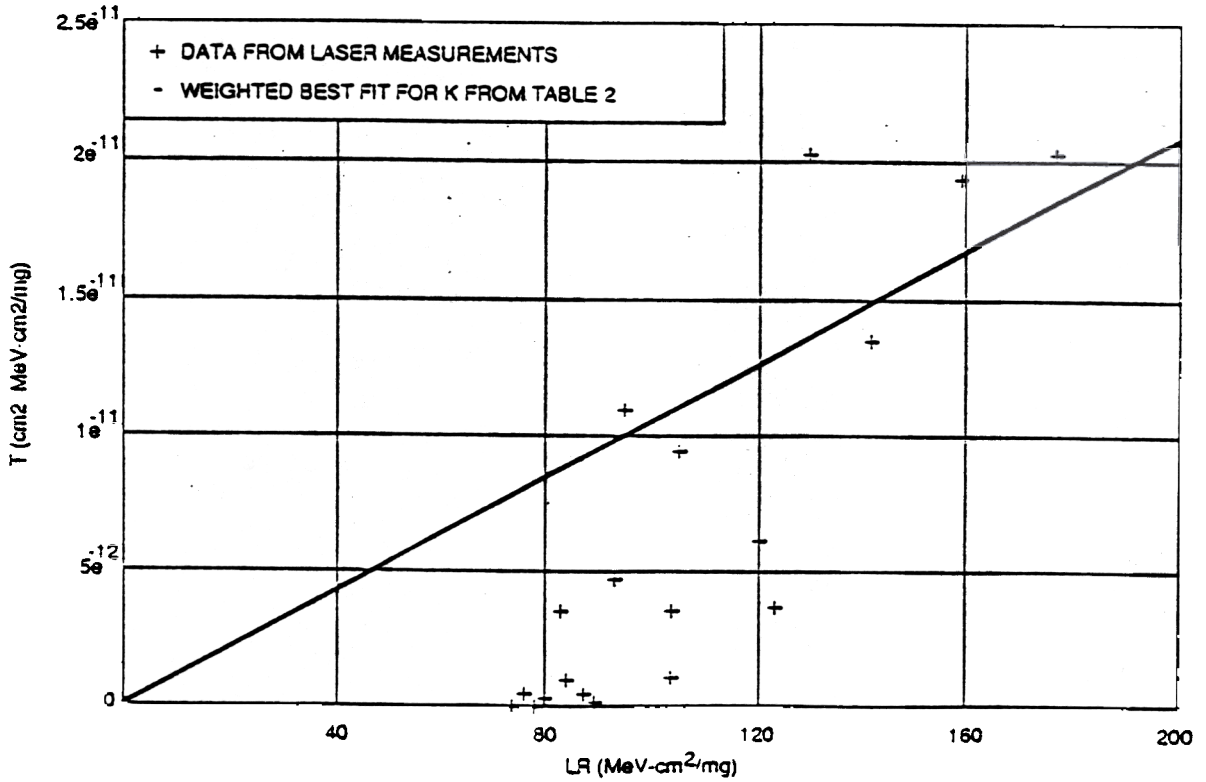

Figure 7. T versus L_R plot of laser data with a solid line indicating the maximum limit of the data.

Table 2. Number of Upsets Versus Pulse Energy and Bias Voltage (Data Used for Figure 6)

Bias Voltage (V_{DD}, Volts)	Pulse Energy (E)					
	1	0.9	0.8	0.7	0.6	0.54
3.0	19	18	14	6	3	1
4.0	19	9	6	2	1	-
5/-	11	7	6	2	-	-
5.5	13	3	0	-	-	-
where E = 79 MeV, α = 3.1 x 10^3/cm, n = 2.24 x $10^{-2}\mu m^{-2}$ and $r = \infty$						

using a laser wavelength of 652 nm. Each datum represents an average of more than 20 measurements. The device contains many structures and can have many different responses depending on where the laser pulse or ion hits. It is assumed that any hits producing less than the maximum number of upsets involve complex interactions and that the simple diffusion model will best fit the data points associated with the largest number of upsets. Therefore, the straight line shown in Figure 7 was used to estimate the slope of the curve. Combining this slope with (9a) produces the estimate

$$2\Pi D^* K = 9.52 \times 10^{12}\ \text{cm}^{-2}$$

With an estimate of K available, it is possible to plot L_R versus N_u for heavy ions via Eq. (12). A plot was made for krypton and is shown in Figure 8. Table 3 contains all data used to produce the predicted curve. Also shown in Figure 8 is the measured heavy-ion response taken from [4,5,6]. For each L_R, the measured number of upsets is the maximum number seen in the histograms of [4,5,6]. The measured points agreed very well in the L_R coordinate of the predicted curve. Note that this comparison was

Table 3. Data for Predicted Points in Figure 7.

$$2\Pi D^* K = 9.52 \times 10^{12}\ \text{cm}^{-2}$$
$$r = 35\ \mu\text{m}$$
$$n = 2.24 \times 10^{-2}\ \mu\text{m}^{-2}$$
$$r = \infty$$

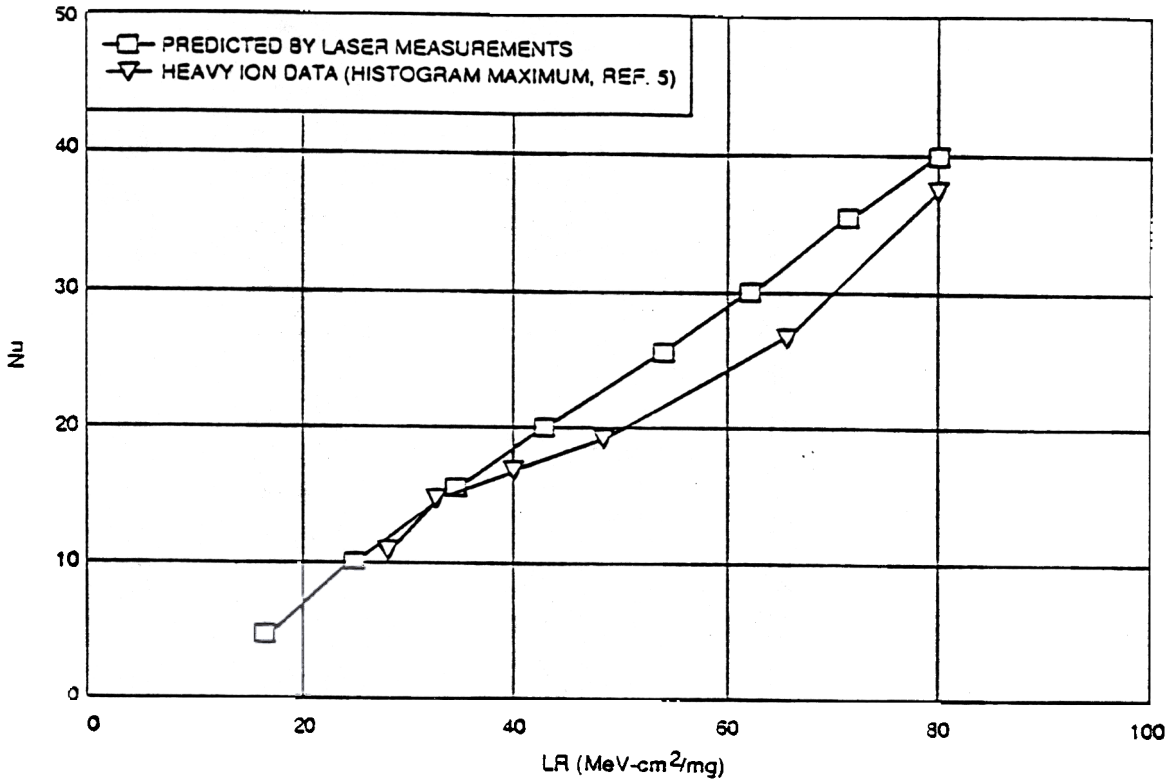

Figure 8. N_u versus L_R for heavy ions.

made based on the assumption that the upsets resulted only from the diffusion of the carriers, which were generated by the picosecond pulsed laser wavelength of 652 nm. In reality, the assumption may not be true. However, these results show a way to analyze a complicated device performance leading to reliability and quality assurance of the device.

C. SIGNIFICANCE OF THE RESULTS

This work demonstrates the unique response characteristics of a NMOS DRAM to different laser wavelengths and intensities. LAMEALS can be used to cost-effectively prescreen ICs for relative SEU sensitivities. Furthermore, the technique can be focused on specific sensitive areas to determine the effectiveness of a particular design by using different laser wavelengths with different penetration depths. A correlation between laser and heavy-ion response was observed.

It is expected that the correlation will improve as theory and calibration methods improve. The ability to optically prebias a circuit with background-light irradiation of varying penetration depths enables this technique to become a direct, real-time diagnostic tool for microelectronic devices.

D. ACKNOWLEDGEMENTS

The authors are grateful to their numerous colleagues for providing technical information for this paper including C. E. Barnes, J. R. Cross, E. F. Cuddihy, L.D. Edmonds, H. G. Garrett. J. O. Okuno, R. P. Ruiz. H. R. Schwartz, L. S. Smith, J. C. Tran, D. T. Vu, K. R. Watson, and J. A. Zoutendyk.

The research described in this paper was carried out by the Center for Space Microelectronics Technology, Jet Propulsion Laboratory, California Institute of Technology, under a contract with the National Aeronautics and Space Administration. Reference herein to any specific commercial product, process, or service by trade name, trademark, manufacturer, or otherwise, does not constitute or imply endorsement by the United States Government or the Jet Propulsion Laboratory, California Institute of Technology.

E. PUBLICATIONS

[1] Q. Kim, G. A. Soli, H. R. Schwartz, J. A. Zoutendyk, L D. Edmonds, D. T. Vu, L S. Smith, and C. E. Barnes, "Picosecond Dye Laser Simulation of Cosmic Ray Effects in NMOS DRAM," llh Symposium on Single-Evenl EffectS, Los Angeles, ApriJ 1990.

[2] Q. Kim, G. A. Soli and H. R. Schwartz, "Microelectronic Advanced Laser Scanner ('MEALS)," new technology transmittal, 1990.

[3] Q. Kim, "Light-Assisted Microelectronic Advanced Laser Scanner (LAMEAlS)," new technology transmittal, 1990.

F. REFERNECES

[1] S. P. Buchner, D. Wilson, K. Kang, D. Gill, *I.* A Mazer, W. D. Raburn, A. B. Campbell, and A. R. Knudson, "Laser Sjmulation of Single-Event UpsetS," *IEEE Transactions on Nuclear Science,* Vol. NS-34, No.6, p. 1228, December 1987.

[2] A K. Richter and I. Arimura, "Simulation of Heavy-Charged Particle Tracks Using Focused Laser Beams," *IEEE Transactions on Nuclear Science,* Vol. NS-34, Pt. I, p. 1234, December 1987.

[3] T.L Criswell, D.L Oberg, J.L. Wert, P.R. Measel, and W. E. Wilson, "Measurement of SEU Thresholds and Cross Sections at Fixed Incidence t..ngles," *IEEE Transactions on Nuclear Science,* Vol. NS-34, No.6, p. 1316, December 1987.

[4] J. A. Zoutendyk, H. R. Schwartz, and L R. NevilI, "Lateral Charge Transport
from Heavy-Ion Tracks in Integrated Circuit Chips," *IEEE TraJtSacliollS on Nuclear Science,* Vol. NS-35, Pt. 1, p. 1644, December 1988.

[5] J. A. Zoutendyk, L. D. Edmonds, and L. S. Smith, "Characterization of Multiple- Bit Errors from Single-Ion Tracks in Integrated Circuits," *IEEE Transactiol1.S on Nuclear Science,* Vol. NS-36, Pt. 1, p. 2267, December 1989.

[6] J. A. Zoutendyk, "Accelerators for Critical Experiments Involving Single-Particle Upset in Solid-State Microcircuits," *Nuclear Instnunents and jYfethods in Physics Research,* Vol. B10, No.11, p. 757, 1985.

[7] G. Arlken, *Malllemarical Method/or PhysicistS,* Znd Edition, Academic Press, p. 760, 1970.